Bioorganic & Medicinal Chemistry 20 (2012) 2427–2434

Contents lists available at SciVerse ScienceDirect

Bioorganic & Medicinal Chemistry

journal homepage: www.elsevier.com/locate/bmc

Optimization of the aromatase inhibitory activities of pyridylthiazole analogues of resveratrol

Abdelrahman S. Mayhoub [a,†], Laura Marler [b], Tamara P. Kondratyuk [b], Eun-Jung Park [b], John M. Pezzuto [b], Mark Cushman [a,*]

[a] Department of Medicinal Chemistry and Molecular Pharmacology, College of Pharmacy, and the Purdue Center for Cancer Research, Purdue University, West Lafayette, IN 47907, United States
[b] College of Pharmacy, University of Hawaii at Hilo, Hilo, HI 96720, United States

ARTICLE INFO

Article history:
Received 2 October 2011
Revised 18 January 2012
Accepted 26 January 2012
Available online 11 February 2012

Keywords:
Aromatase
Inhibitor
Resveratrol
Chemotherapy
Chemoprevention

ABSTRACT

Aromatase is an established target not only for breast cancer chemotherapy, but also for breast cancer chemoprevention. The moderate and non-selective aromatase inhibitory activity of resveratrol (**1**) was improved about 100-fold by replacement of the ethylenic bridge with a thiadiazole and the phenyl rings with pyridines (e.g., compound **3**). The aromatase inhibitory activity was enhanced over 6000-fold by using a 1,3-thiazole as the central ring and modifying the substituents on the 'A' ring to target the Met374 residue of aromatase. On the other hand, targeting the hydroxyl group of Thr310 by a hydrogen-bond acceptor on the 'B' ring did not improve the aromatase inhibitory activity.

1. Introduction

Breast cancer is the most common cancer in the world. It is still the most frequent cancer among females and it is the second leading cause of death from cancer in women.[1] There were 192,370 cases of invasive breast cancer reported in the United States in 2009.[2] The vast majority of both pre- and postmenopausal breast cancers are classified as estrogen-dependent.[3]

Normally estrogens control the development and maintenance of the female sex organs, secondary sex characteristics, mammary glands, and certain functions of the uterus and its accessory organs. The pathological effect of the estrogens, as in the case of estrogen-dependent breast cancer, occurs when the tumor cells express excess receptors for endogenous estrogens. The binding of estrogen to its receptor activates transcription of its target genes, which are responsible for cancer cell proliferation.[4] Therefore, clinical treatment focuses on decreasing the amount of estrogens either by oophorectomy[5] or blocking the pathological effect of endogenous estrogens by using anti-estrogen chemotherapy. One anti-estrogen therapeutic modality involves the use of aromatase inhibitors, including both steroidal[6] and non-steroidal derivatives.[7] Since the mid-1990s, a third generation of non-steroidal aromatase inhibitors has became available that has shown therapeutic superiority over steroidal derivatives.[8] There are different classes of non-steroidal aromatase inhibitors, including benzoflavanones,[9] azoles and azines,[10] and stilbene derivatives, which display both anticancer[11] and cancer chemopreventive effects.[12]

Resveratrol (**1**) is a natural stilbene derivative that occurs in various edible plants such as grapes and nuts.[13] It has several therapeutic effects including improving postischemic ventricular performance[14] and cancer[15] chemopereventive activities. However, resveratrol exerts its chemopreventive effect via modulating many biological pathways that are potentially capable of inhibiting carcinogenesis, and it has relatively low potency in each. In addition, it is metabolized rapidly into inactive metabolites.[16] For these reasons, there is a need to investigate other resveratrol derivatives that might show greater efficacy and selectivity.

This report describes recent efforts to develop more potent and selective resveratrol cancer chemopreventive analogues. The resveratrol trans stilbene double bond was previously replaced with a thiadiazole ring.[17] This strategy afforded the lead compound **2** that had some chemopreventive activity against aromatase and NF-κB, and a good induction ratio with NAD(P)H:quinone reductase (QR1).[17] Further chemical optimization of the lead compound **2** furnished 3,5-dipyridyl-1,2,4-thiadiazoles (e.g., compound **3**) as a

Abbreviations: IC_{50}, sample concentration which causes 50% inhibition; iNOS, inducible nitric oxide synthase; NF-κB, nuclear factor kappa-light-chain-enhancer of activated B cells; QR1, NAD(P)H:quinone reductase.

* Corresponding author.
E-mail address: cushman@purdue.edu (M. Cushman).
† On leave from Al-Azhar University, College of Pharmacy, Cairo, Egypt.

0968-0896/$ - see front matter © 2012 Elsevier Ltd. All rights reserved.
doi:10.1016/j.bmc.2012.01.047

new class of non-steroidal aromatase inhibitors.[17] More attention has recently been given to improve the aromatase inhibitory activity of this newly discovered class of aromatase inhibitors since aromatase is an established target in both breast cancer chemotherapy[18] and chemoprevention.[16]

group or a halogen. The *para* position of the 'B' ring is calculated to be 3.9 Å away from the hydroxyl group of Thr310 (Fig. 1), so instillation of hydrogen-bond acceptors, such as a methoxy group or halogens, might increase potency. In the same molecular model (Fig. 1), the *ortho* position of the 'A' ring is close to a hydrophobic

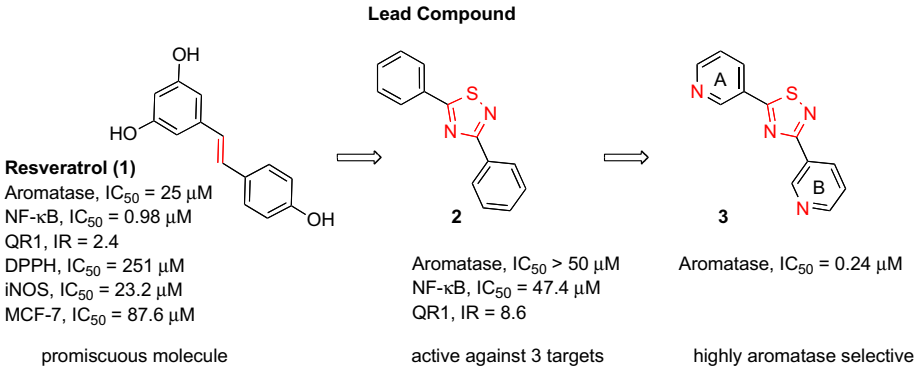

The two peripheral rings are arbitrarily denoted "A" and "B" in structure **3**.

All of the target compounds were tested for their aromatase inhibitory activity. Resveratrol (**1**) and three clinically used non-steroidal aromatase inhibitors were also tested as positive controls. In addition, to test the chemopreventive selectivity of the compounds, they were also evaluated against other enzymes that are involved in chemopreventive pathways, such as NF-κB, inducible nitric oxide synthase (iNOS), and QR1 (see Supplementary data).

2. Results and discussion

2.1. Chemistry

To further enhance the aromatase inhibitory activity of compound **3**, a structure-based design strategy was adopted and compound **3** was docked into the active site of aromatase (PDB ID 3eqm)[19] using GOLD software.[20] The hypothetical model of the binding of compound **3** with aromatase is represented in Figure 1, which shows the possible interaction between the pyridine nitrogen of the 'A' ring and the heme iron, while the other nitrogen is calculated to hydrogen bond with the NH of Met374. The model suggests several strategies to increase the aromatase inhibitory potency. First, the nitrogen atom of the 'A' ring of compound **3** is near to the NH group of Met374, suggesting replacement of the nitrogen of the ligand by other hydrogen-bond acceptors, such as a methoxy

region (Leu477). Therefore, a small hydrophobic group is anticipated to improve the hydrophobic interactions. All of the suggested modifications are summarized in Figure 2.

Although there are abundant methods reported for synthesis of 3,5-disubstituted-1,2,4-thiadiazoles with identical substituents,[21] there are limited ones for those with non-identical substituents.[22] To prepare 3,5-disubstituted-1,2,4-thiadiazoles **6a** and **b**, Howe's method[22] was followed and oxathiazolone **5**, prepared from nicotinamide (**4**) and (chlorocarbonyl)sulfenyl chloride, was allowed to react with 3-bromobenzonitrile and its 3-methoxy analogue in decalin at 200 °C (Scheme 1).

Appropriate thioamides **8a–f** were allowed to react with bromoacetylpyridine hydrobromide **7** in dry DMF to afford the desired thiazoles **9a–f** (Scheme 2). The hydroxyl derivative **9g** was obtained from its corresponding methoxy analogue **9e** by treatment with hydrogen bromide in refluxing glacial acetic acid.

Compound **11** was prepared from thioamide **10** and bromoacetylpyridine **7** as shown in Scheme 3. The methoxy derivative **12** was obtained by allowing compound **11** to react with 10 equiv sodium methoxide and absolute methanol in a sealed tube at 120 °C.

Heating 3,4-dimethylpyridine (**13**) with selenium dioxide in dioxane afforded the corresponding aldehyde **14** as outlined in Scheme 4. The aldehyde was converted directly into its corresponding amide using the Chill and Mebane method.[23] The amide

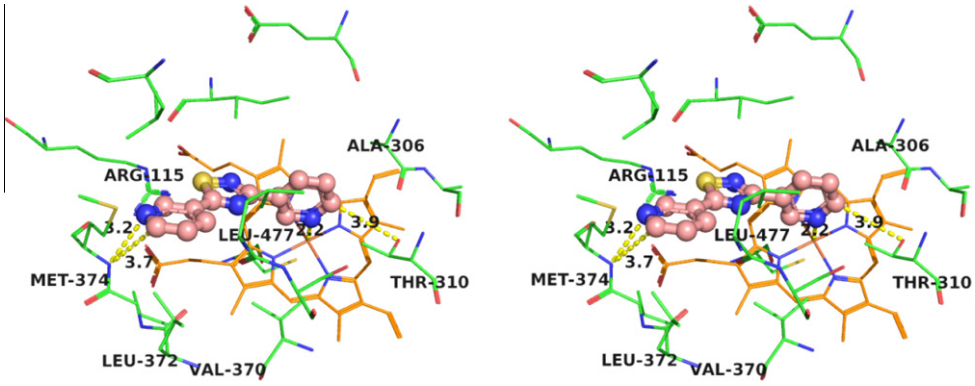

Figure 1. Hypothetical interaction between compound **3** and Met374 and heme in the human aromatase active site (PDB ID 3eqm). The stereoview is programmed for wall-eyed viewing.

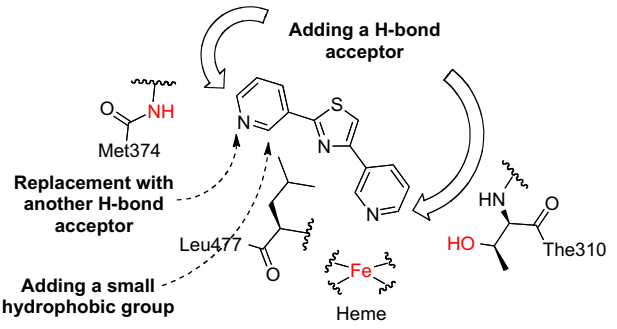

Figure 2. Design of novel analogues to compound **3** based on its docking results.

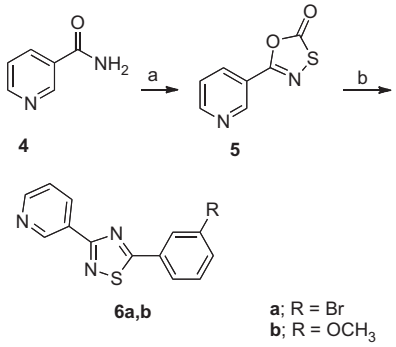

Scheme 1. Reagents and conditions: (a) (chlorocarbonyl)sulfenyl chloride, toluene, heat to reflux, 24 h, 31%; (b) 3-bromobenzonitrile or 3-methoxybenzonitrile, decalin, 200 °C, 20 min, 8–13%.

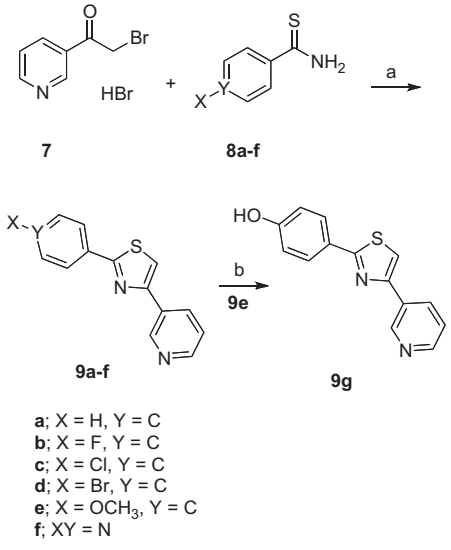

Scheme 2. Reagents and conditions: (a) DMF, Cs_2CO_3, heat to reflux, 3–6 h, 70–80%; (b) (i) HBr, acetic acid, heat to reflux; (ii) K_2CO_3, 24 h, 44%.

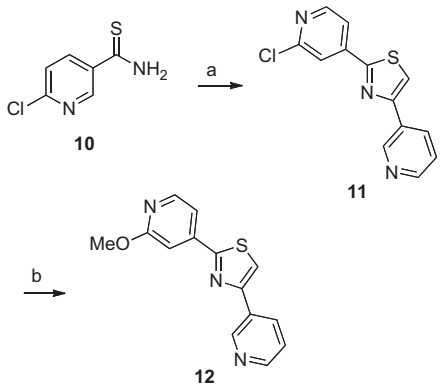

Scheme 3. Reagents and conditions: (a) 2-bromoacetyl-3-pyridine hydrobromide (**7**), DMF, Cs_2CO_3, 100 °C, 8 h, 67%; (b) NaOMe, MeOH, 120 °C, 24 h, 98%.

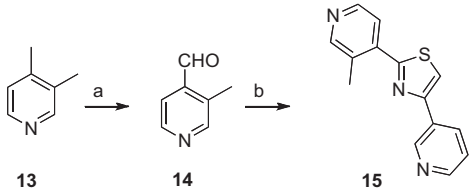

Scheme 4. Reagents and conditions: (a) SeO_2, dioxane, 100 °C, 12 h, 80%; (b) (i) $NH_2OH{\cdot}HCl$, DMSO, 100 °C, 30 min; (ii) NaOH, H_2O_2, 100 °C, 7 min, 70%; (iii) Lawesson's reagent, THF, 50 °C, 3 h, 54%; (iv) 2-bromoacetyl-3-pyridine hydrobromide (**7**), DMF, Cs_2CO_3, 100 °C, 8 h, 56%.

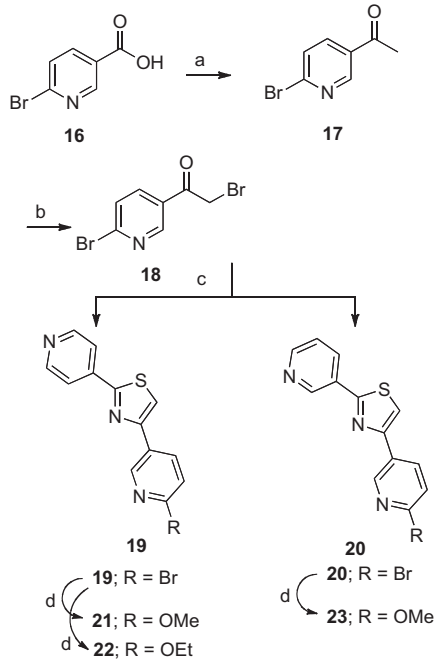

Scheme 5. Reagents and conditions: (a) MeMgBr (2 equiv), dry THF, 23 °C, 10 min, 100%; (b) bromine, CCl_4, heat to reflux, 3 h, 5%; (c) thionicotinamide or thioisonicotinamide, DMF, Cs_2CO_3, heat to 120 °C, 6 h; 55–57%; (d) NaOMe, MeOH or EtOH, 120 °C 46–58%.

was treated with Lawesson's reagent in dry THF to yield a yellow solid identified as 3-methylpyridine-4-carbothioamide, which was treated with 2-bromoacetyl-3-pyridine hydrobromide (**7**) as described in Scheme 2 to afford the desired thiazole **15** (Scheme 4).

3-Acetylpyridine **17** was obtained from the commercially available pyridine-3-carboxylate **16** using 2 equiv methyl magnesium bromide (Scheme 5). Compound **17** was heated in CCl_4 with bromine to afford the corresponding monobromoacetyl derivative **18** in low yield. Changing the solvent from CCl_4 to glacial acetic acid or acetonitrile or the brominating agent from elemental bromine

to NBS did not improve the yield. Compound **18** was allowed to react with the suitable pyridine thioamides to afford 6-bromopyridylthiazoles **19** and **20** (Scheme 5). The desired methoxypyridine derivatives **21** and **23** were obtained by heating their corresponding bromo analogues **19** and **20** with 5 equiv sodium methoxide and absolute methanol in a sealed tube. Using absolute ethanol as solvent under the same experimental conditions afforded the ethoxy derivative **22** as the only isolable product (Scheme 5).

2.2. Biological results

First, thiadiazole derivatives **6a** and **6b** were prepared and both showed weaker aromatase inhibitory activity than compound **3** (Table 1). This observed decrease in the anti-aromatase activity might be due to the size congestion. The targeted Met374 NH group appears to be closer to the 'A' ring *meta* position, but it is also close enough to the *para* position for that to be considered. Therefore, the attachment of hydrogen-bond acceptors to the 'A' ring *para* position was considered. Originally, it was decided to perform the aforementioned chemical modifications using a thiadiazole central ring, but after the experience of preparation of compounds **6a** and **6b**, it was clear that synthesis of thiadiazoles with two non-identical substituents in the required purity and enough quantities would be difficult. For these reasons and since the thiadiazole nitrogen at the 2-position apparently has no role in the interaction with active site residues as shown in Figure 1, the thiadiazole central ring was replaced with a thiazole ring and all subsequent modifications were performed using a 2,4-diaryl-1,3-thiazole scaffold.

Using this new framework provided higher accessibility and a more feasible chemical pathway. Thiazole derivatives **9a–g** with different 'A' ring *para* substitutions were prepared and tested for their aromatase inhibitory activity. Among this set of compounds, the 4-pyridyl derivative **9f** showed significantly greater inhibitory activity with an IC_{50} value of 4 nM (Table 1) and a K_i value of 60 pM (Table 1, Fig. 3). These values are comparable with those of the clinically available non-steroidal aromatase inhibitors letrozole, anastrozole and fadrozole (Table 1), suggesting this compound is a good drug candidate. As mentioned earlier, all compounds were subjected to a range of chemopreventive assays to test their target selectivity. Compound **9f** had moderate NF-κB inhibitory activity with an IC_{50} of 2.5 μM.

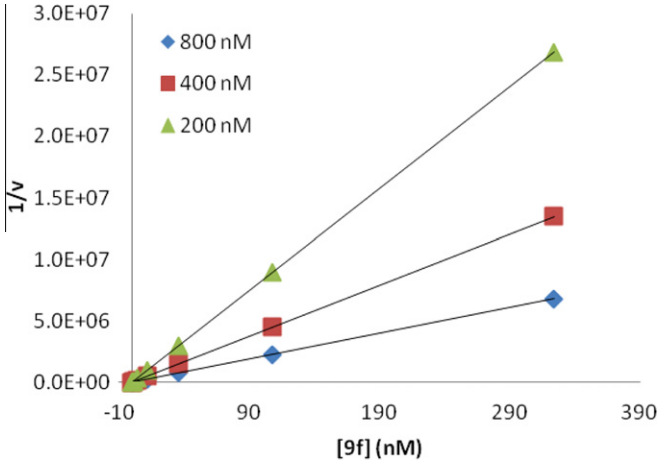

Figure 3. Dixon plot illustrating the inhibition of aromatase by compound **9f**.

Additional compounds were made and tested in an effort to further probe the structure–activity-relationships. Hydrogen-bond acceptor moieties were added to the 'A' ring *meta* position and compounds **11** and **12** were prepared. Both compounds displayed aromatase IC_{50} values (164 and 23 nM, respectively) that were better than the lead compound in this study, that is, compound **2**, as shown in Table 1. Compound **12** had a higher aromatase IC_{50} value (23 nM) than compound **9f**, but it had complete aromatase target selectivity, being inactive vs. quinone reductase 1, NF-κB, and nitric oxide synthase (see Supplementary data). Figure 4 represents the hypothetical binding mode of compound **12** within the aromatase active site. The nitrogen atom of the 'B' ring is calculated to be very close to the heme iron, similar to what is observed in case of the lead compound **3** (Fig. 1). In contrast, the nitrogen atom of the 'A' ring was calculated to be displaced 2.7 Å away from the Met374 NH group. Instead, the methoxy group of the 'A' ring was hypothetically docked 3.3 Å close to the Met374 NH group, which suggesting a possibility of a hydrogen bond between the Met374 NH and the oxygen atom of compound **12** methoxy group. This observation might explain why compound **12** has weaker aromatase inhibitory activity than **9f**.

The last chemical modification on the 'A' ring resulted in compound **15**. In the molecular model (Fig. 1), the *ortho* position of the 'A' ring is close to a hydrophobic region (Leu477). Therefore, a small hydrophobic group was added to the structure of compound **9f** and that furnished its *o*-methyl analogue **15**. Although compound **15** had an aromatase IC_{50} value in the nanomolar range (IC_{50} 78 nM, Table 1), it was higher than that of **9f**. The observed decrease in the aromatase inhibitory potency might be because introduction of an *o*-methyl in the 'A' ring pushes the molecule closer to Arg115 (Fig. 5); as a result, the nitrogen atom of the 'B' ring shifted a little farther away from the heme iron.

Next, chemical modifications of the 'B' ring were considered. A hydrogen-bond acceptor moiety was designed to be added to the 'B' ring in the *para* position in order to target the Thr310 hydroxy group (Fig. 1). Since in the 'A' ring, nitrogen atoms at position-3 and position-4 have biological significance, both were taken into consideration and the 'B' ring chemical modifications were performed using both systems. Therefore, *p*-bromo and their alkoxy derivatives **19–23** were prepared. This set of compounds showed higher aromatase maximum percent inhibition than **9f** when measured at 20 μM, but the IC_{50} values ranged between 0.59 and 7.41 μM (Table 1).

Table 1
Inhibition of human aromatase by thiadiazoles and their thiazole analogues[a]

Compound	IC_{50}[a] (μM)	K_i[b] (nM)
3	0.24 ± 0.08	11.43 ± 0.91
6a	6.73 ± 0.21	1160 ± 2.6
6b	14.9 ± 0.33	5321 ± 22
9a	0.9 ± 0.04	63.38 ± 5.3
9b	17.58 ± 0.47	12560 ± 34
9c	2.39 ± 0.26	234.3 ± 8.6
9d	7.92 ± 0.15	1722 ± 5.4
9e	18 ± 0.38	15000 ± 48
9f	0.004 ± 0.0005	0.06 ± 0.04
9g	11.21 ± 0.27	2548 ± 15
11	0.164 ± 0.06	8.20 ± 0.73
12	0.023 ± 0.004	0.65 ± 0.07
15	0.078 ± 0.007	3.17 ± 0.22
19	2.68 ± 0.36	285.1 ± 4.5
20	7.41 ± 0.42	1482 ± 9.2
21	1.04 ± 0.19	82.54 ± 7.1
22	1.36 ± 0.24	100.0 ± 2.8
23	0.59 ± 0.11	35.12 ± 1.6
Resveratrol (1)	25 ± 0.52	41670 ± 27
Letrozole	0.002 ± 0.0004	0.02 ± 0.01
Anastrozole	0.008 ± 0.0007	0.13 ± 0.04
Fadrozole	0.003 ± 0.001	0.05 ± 0.008

[a,b] IC_{50} (μM) and K_i (nM) values are summarized for each of the tested compounds. In each case, competitive inhibition was observed.

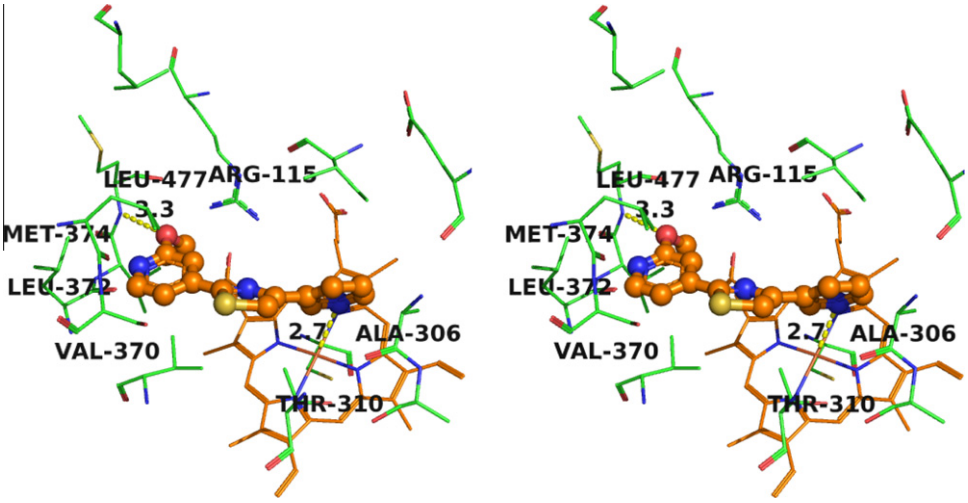

Figure 4. Hypothetical interaction between compound **12** and Met374 and heme in the human aromatase active site (PDB ID 3eqm). The stereoview is programmed for wall-eyed viewing.

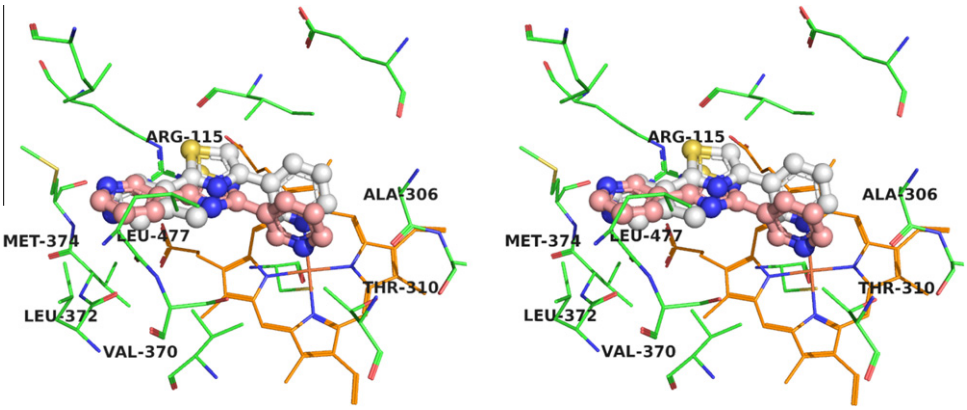

Figure 5. Overlay of the top calculated binding poses of compounds **3** and **15** in the human aromatase active site (PDB ID 3eqm). C-Backbone of compound **3** was colored pink, and compound **15** was colored gray. The stereoview is programmed for wall-eyed viewing.

3. Conclusion

Use of a 2,4-diaryl-1,3-thiazole scaffold provided more flexible synthetic pathways to build novel aromatase inhibitors with IC_{50} values in the nanomolar range. Using the new scaffold and optimizing the position of the hydrogen-bond acceptor on the 'A' ring of the lead compound **2** afforded compound **9f**, which had an aromatase IC_{50} value of 4 nM. In addition to the potent aromatase inhibitory activity of compound **9f**, moderate NF-κB inhibitory activity was also observed. The methoxy derivative **12** provided complete aromatase inhibitory selectivity with potency in the low nanomolar range (IC_{50} 23 nM).

4. Experimental section

4.1. General

^{1}H NMR spectra were recorded at 300 MHz and ^{13}C NMR spectra were acquired at 75.46 MHz in deuterated chloroform ($CDCl_3$) or dimethyl sulfoxide (DMSO-d_6). Chemical shifts are given in parts per million (ppm) on the delta (δ) scale. Chemical shifts are related to that of the solvent. Mass spectra were recorded at 70 eV. High resolution mass spectra for all ionization techniques were obtained from a FinniganMAT XL95. Melting points were determined using capillary tubes with a Mel-Temp apparatus and are uncorrected. HPLC analyses were performed on a Waters binary HPLC system (Model 1525, 20 μL injection loop) equipped with a Waters dual wavelength absorbance UV detector (Model 2487) set for 254 nm, using a 5 μM C-18 reverse phase column. Compounds **9f**,[24] **10**,[25] **14**,[26] **16**,[27] and **17**[28] are reported.

4.2. 5-(Pyridin-3-yl)-1,3,4-oxathiazol-2-one (5)

Nicotinamide (**4**, 490 mg, 4.0 mmol) was added to (chlorocarbonyl)sulfenyl chloride (780 mg, 6.39 mmol) in toluene (30 mL). The reaction mixture was heated at reflux for 24 h. The solution was allowed to cool and solvent was evaporated under reduced pressure. The brown solid was collected and crystallized from ethyl acetate to provide the required products as a yellowish solid (223 mg, 30.9%): mp 117–118 °C. ^{1}H NMR ($CDCl_3$) δ 9.09 (d, J = 1.8 Hz, 1H), 8.71 (dd, J = 1.5, 4.8 Hz, 1H), 8.16 (dt, J = 1.8, 7.8 Hz, 1H), 7.39 (dd, J = 4.5, 7.8 Hz, 1H); ^{13}C NMR ($CDCl_3$) δ 172.89, 155.29, 153.02, 148.40, 134.44, 123.65, 122.02; CIMS *m/z* (rel intensity) 181 (MH^+, 26), 106 (100); HRMS (EI), *m/z* 179.9991 M^+, calcd for $C_7H_4N_2O_2S$ 179.9994.

4.3. Preparation of thiadiazoles 6a,b

Oxathiazolone **5** (90 mg, 0.5 mmol) was added in portions, over a 10 min time period, to a stirred solution of 3-bromobenzonitrile

or 3-methoxybenzonitrile (5.0 mmol) in decalin (5 mL) at 200 °C. The reaction mixture was stirred for an additional 10–15 min, and then cooled to room temperature. The products were separated and purified by silica gel flash chromatography, using hexane–ethyl acetate (4:1).

4.3.1. 5-(3-Bromophenyl)-3-(pyridin-3-yl)-1,2,4-thiadiazole (6a)

White solid (20.5 mg, 12.8%): mp 120 °C. ^{1}H NMR ($CDCl_3$) δ 9.59 (s, 1H), 8.72 (d, J = 3.3 Hz, 1H), 8.62 (dt, J = 1.8, 7.5 Hz, 1H), 9.22 (d, J = 1.6 Hz, 1H), 7.95 (d, J = 7.8 Hz, 1H), 7.67 (dd, J = 1.0, 7.8 Hz, 1H), 7.41 (m, 2H); ^{13}C NMR ($CDCl_3$) δ 186.99, 171.42, 151.18, 149.67, 135.43, 134.97, 132.05, 130.83, 130.17, 128.43, 126.10, 123.53, 123.41; CIMS *m/z* (rel intensity) 320/318 (MH^+, 25/25), 105 (100); HRMS (EI), *m/z* 316.9625 M^+, calcd for $C_{13}H_8BrN_3S$ 316.9622; HPLC purity (C-18 reverse phase column): 95.97% (methanol–H_2O, 95:5).

4.3.2. 5-(3-Methoxyphenyl)-3-(pyridin-3-yl)-1,2,4-thiadiazole (6b)

White solid (11 mg, 8.1%): mp 122–123 °C. ^{1}H NMR ($CDCl_3$) δ 9.63 (s, 1H), 8.73 (s, 1H), 8.65 (dd, J = 2.0, 7.8 Hz, 1H), 8.16 (dd, J = 3.5, 7.8 Hz, 1H), 7.64 (d, J = 7.8 Hz, 1H), 7.46–7.44 (m, 2H), 6.98 (dd, J = 3.0, 8.1 Hz, 1H), 3.93 (s, 3H); ^{13}C NMR ($CDCl_3$) δ 185.32, 168.94, 159.02, 150.94, 149.62, 135.37, 134.72, 132.11, 128.41, 123.57, 119.40, 115.24, 114.08, 55.74; CIMS *m/z* (rel intensity) 270 (MH^+, 40), 136 (100); HRMS (CI), *m/z* 270.0698 MH^+, calcd for $C_{14}H_{12}N_3OS$ 270.0696; HPLC purity (C-18 reverse phase column): 95.02% (methanol–H_2O, 95:5).

4.4. Preparation of thiazole derivatives 9a–e

Thioamides **8a–f** (0.5 mmol), 3-(bromoacetyl)pyridine hydrobromide (**7**, 140 mg, 0.50 mmol), and cesium carbonate (165 mg, 0.51 mmol) were added to dry DMF (10 mL). The reaction mixture was heated to reflux for 3–6 h and then allowed to cool, quenched with water (20 mL), and filtered. The solid residues were purified by silica gel flash chromatography, using hexane–ethyl acetate (4:1).

4.4.1. 2-Phenyl-4-(pyridin-3-yl)thiazole (9a)

Off-white solid (83 mg, 70%): mp 82–83 °C. ^{1}H NMR ($CDCl_3$) δ 9.18 (s, 1H), 8.56 (d, J = 3.6 Hz, 1H), 8.24 (d, J = 7.8 Hz, 1H), 8.01 (m, 2H), 7.51 (s, 1H), 7.44–7.26 (m, 3H), 7.33 (m, 1H); ^{13}C NMR ($CDCl_3$) δ 168.54, 152.99 (2C), 148.94, 147.62, 133.69, 133.29, 130.29, 128.96 (2C), 126.56 (2C), 123.60, 113.82; ESIMS *m/z* (rel intensity) 239 (MH^+, 100); HRMS (ESI), *m/z* 239.0641 MH^+, calcd for $C_{14}H_{11}N_2S$ 239.0637; HPLC purity (C-18 reverse phase column): 97.54% (methanol–H_2O, 95:5).

4.4.2. 2-(4-Fluorophenyl)-4-(pyridin-3-yl)thiazole (9b)

Yellowish-white solid (97 mg, 76%): mp 141–142 °C. ^{1}H NMR ($CDCl_3$) δ 9.18 (s, 1H), 8.56 (d, J = 4.5 Hz, 1H), 8.24 (d, J = 7.5 Hz, 1H), 7.99 (dd, J_{HH} = 4.8 Hz, J_{HF} = 7.8 Hz, 2H), 7.52 (s, 1H), 7.35 (dt, J = 4.5, 7.8 Hz, 1H), 7.13 (dd, J_{HH} = 4.5, J_{HF} = 7.8 Hz, 2H); ^{13}C NMR ($CDCl_3$) δ 167.29, 165.61, 162.29, 153.10, 149.15, 147.72, 133.59, 130.09 (d, J_{CF} = 32.2 Hz, 1C), 128.43 (d, J_{CF} = 7.5 Hz, 2C), 123.53, 116.17 (d, J_{CF} = 22.0 Hz, 2C), 113.67; ESIMS *m/z* (rel intensity) 257 (MH^+, 100); HRMS (ESI), *m/z* 257.0545 MH^+, calcd for $C_{14}H_{10}FN_2S$ 257.0543; HPLC purity (C-18 reverse phase column): 98.89% (methanol–H_2O, 95:5).

4.4.3. 2-(4-Chlorophenyl)-4-(pyridin-3-yl)thiazole (9c)

Yellowish-brown solid (102 mg, 75.0%): mp 141–142 °C. ^{1}H NMR ($CDCl_3$) δ 9.15 (s, 1H), 8.56 (s, 1H), 8.19 (d, J = 7.8 Hz, 1H), 7.87 (d, J = 8.7 Hz, 2H), 7.49 (s, 1H), 7.32 (m, 3H); ^{13}C NMR ($CDCl_3$) δ 167.06, 153.17, 149.11, 147.64, 136.16, 133.58, 131.73, 130.02, 129.12 (2C), 127.69 (2C), 123.58, 113.97; ESIMS *m/z* (rel intensity) 331 (MH^+, 100); HRMS (ESI), *m/z* 273.0253 MH^+, calcd for $C_{14}H_{10}ClN_2S$ 273.0248; HPLC purity (C-18 reverse phase column): 98.19% (methanol–H_2O, 95:5).

4.4.4. 2-(4-Bromophenyl)-4-(pyridin-3-yl)thiazole (9d)

Yellowish-brown solid (125 mg, 79.5%): mp 100 °C. ^{1}H NMR ($CDCl_3$) δ 9.13 (s, 1H), 8.55 (d, J = 4.6 Hz, 1H), 8.17 (d, J = 7.8 Hz, 1H), 7.89 (d, J = 8.7 Hz, 2H), 7.51 (s, 1H), 7.48 (d, J = 8.7 Hz, 2H), 7.29 (m, 1H); ^{13}C NMR ($CDCl_3$) δ 167.07, 153.17, 149.15, 147.67, 133.55, 132.13, 132.05, 129.94 (2C), 127.88 (2C), 124.51, 123.53, 113.99; ESIMS *m/z* (rel intensity) 319/317 (MH^+, 96/100); HRMS (ESI), *m/z* 316.9752 MH^+, calcd for $C_{14}H_{10}BrN_2S$ 316.9748; HPLC purity (C-18 reverse phase column): 95.27% (methanol–H_2O, 95:5).

4.4.5. 2-(4-Methoxyphenyl)-4-(pyridin-3-yl)thiazole (9e)

White solid (95 mg, 71%): mp 104 °C. ^{1}H NMR ($CDCl_3$) δ 9.19 (s, 1H), 8.57 (d, J = 3.9 Hz, 1H), 8.26 (d, J = 7.8 Hz, 1H), 7.95 (d, J = 8.7 Hz, 2H), 7.48 (s, 1H), 7.35 (dd, J = 4.4, 7.5 Hz, 1H), 6.97 (d, J = 8.7 Hz, 2H), 3.85 (s, 3H); ^{13}C NMR ($CDCl_3$) δ 168.41, 161.31, 152.80, 148.97, 147.73, 133.61, 130.35, 128.07 (2C), 126.33 (2C), 123.52, 114.26, 112.87, 55.39; ESIMS *m/z* (rel intensity) 269 (MH^+, 100); HRMS (ESI), *m/z* 269.0747 MH^+, calcd for $C_{15}H_{13}N_2OS$ 269.0743; HPLC purity (C-18 reverse phase column): 95.05% (methanol–H_2O, 95:5).

4.4.6. 4-[4-(Pyridin-3-yl)thiazol-2-yl]phenol (9g)

Aqueous HBr (48%, 3 mL) was added to compound **9e** (50 mg, 0.2 mmol) in acetic acid (7 mL). The reaction mixture was heated at reflux for 24 h. After the reaction mixture was cooled down to room temperature, it was neutralized with K_2CO_3 powder until pH 7. The solid was collected by filtration and purified by silica gel flash chromatography, using dichloromethane–methanol (95:5), to afford the product as a white solid (22 mg, 44%): mp 271–273 °C. IR (KBr) 3434, 3045, 1608, 1586, 1472 cm^{-1}; ^{1}H NMR (DMSO-d_6) δ 9.23 (d, J = 1.5 Hz, 1H), 8.55 (d, J = 4.8 Hz, 1H), 8.35 (d, J = 7.8 Hz, 1H), 8.20 (s, 1H), 7.85 (d, J = 8.7 Hz, 2H), 7.48 (dd, J = 4.8, 7.8 Hz, 1H), 6.89 (d, J = 8.7 Hz, 2H), 3.8 (brs, 1H); ^{13}C NMR (DMSO-d_6) δ 168.95, 160.91, 152.74, 149.84, 148.19, 134.19, 130.78, 128.96 (2C), 124.80 (2C), 116.93, 115.46; ESIMS *m/z* (rel intensity) 255 (MH^+, 100); HRMS (ESI), *m/z* 255.0594 MH^+, calcd for $C_{14}H_{11}N_2OS$ 255.0592; HPLC purity (C-18 reverse phase column): 96.90% (methanol–H_2O, 95:5).

4.5. 2-(2-Chloropyridin-4-yl)-4-(pyridin-3-yl)thiazole (11)

Thioamide **10** (60.0 mg, 0.35 mmol), 3-(bromoacetyl)pyridine hydrobromide (**7**, 98 mg, 0.35 mmol), and cesium carbonate (170 mg, 0.52 mmol) were added to dry DMF (10 mL). The reaction mixture was heated at 100 °C for 8 h and then allowed to cool and then quenched with distilled water (30 mL). The organic materials were extracted with ethyl acetate (30 mL). The organic layer was isolated and dried over anhydrous Na_2SO_4. Solvent was evaporated under reduced pressure. The solid residue was purified by silica gel flash chromatography, using ethyl acetate–hexane (1:1), and then dichloromethane–methanol (95:5) to yield a yellowish-white solid (64 mg, 67%): mp 182–183 °C. ^{1}H NMR (DMSO-d_6) δ 9.28 (s, 1H), 8.56 (m, 3H), 8.42 (d, J = 7.2 Hz, 1H), 8.10 (s, 1H), 8.01 (d, J = 7.0 Hz, 1H), 7.52 (dd, J = 3.9, 7.2 Hz, 1H); ^{13}C NMR (DMSO-d_6) δ 164.22, 154.03, 152.41, 152.06, 150.36, 148.35, 143.52, 134.50, 130.11, 124.88, 121.19, 120.72, 120.06; ESIMS (*m/z*, rel intensity) 274/276 (MH^+, 100/24); HRMS (ESI), *m/z* MH^+ 274.0201, calcd for $C_{13}H_8ClN_3S$ 274.0206; HPLC purity (C-18 reverse phase column): 98.93% (methanol–H_2O, 95:5).

4.6. 2-(2-Methoxypyridin-4-yl)-4-(pyridin-3-yl)thiazole (12)

Compound **11** (70.0 mg, 0.25 mmol) and sodium methoxide (140 mg, 2.59 mmol) were added to absolute methanol (3 mL) in a sealed tube. The reaction mixture was heated at 120 °C for 24 h and then allowed to cool. The solvent was evaporated under reduced pressure and the solid residue was partitioned between ethyl acetate (10 mL) and water (10 mL). The organic layer was isolated and dried over anhydrous Na_2SO_4. Solvent was evaporated under reduced pressure and the solid residue was purified by silica gel flash chromatography, using dichloromethane–methanol (95:5), to yield white solid (66 mg, 98%): mp 115–116 °C. ^{1}H NMR ($CDCl_3$) δ 9.16 (s, 1H), 8.58 (s, 1H), 8.23 (d, J = 7.4 Hz, 2H), 7.63 (s, 1H), 7.44 (dd, J = 1.2, 7.4 Hz, 1H), 7.34 (dd, J = 4.5, 7.5 Hz, 1H), 7.30 (s, 1H), 3.97 (s, 3H); ^{13}C NMR ($CDCl_3$) δ 165.63, 164.93, 153.67, 149.37, 147.82, 147.70, 142.53, 133.67, 129.78, 123.60, 115.16, 113.87, 107.64, 53.72; ESIMS (m/z, rel intensity) 270 (MH^+, 100); HRMS (ESI), m/z MH^+ 270.0704, calcd for $C_{14}H_{12}N_3OS$ 270.0701; HPLC purity (C-18 reverse phase column): 95.16% (methanol–H_2O, 95:5).

4.7. 2-(3-Methylpyridin-4-yl)-4-(pyridin-3-yl)thiazole (15)

The aldehyde **14** (800 mg, 6.61 mmol) was added to a solution of hydroxylamine hydrochloride (725 mg, 10.5 mmol) in DMSO (15 mL), and the resulting reaction mixture was stirred and heated for 30 min at 100 °C. The heat was then removed. Sodium hydroxide (600 mg) was dissolved in distilled water (5 mL) and the resulting solution was slowly added to the reaction mixture over a 2-min period with stirring, followed by the slow and careful addition of H_2O_2 (50%, 4 mL) over a 5-min period. The reaction mixture was further stirred for 5 min, quenched with distilled water (30 mL), and then extracted with ethyl acetate (50 mL). The organic layer was separated, dried over anhydrous Na_2SO_4, and evaporated under reduced pressure to afford a white solid (495 mg, 70.4%). The solid (135 mg, 1.00 mmol) and Lawesson's reagent (490 mg, 1.20 mmol) were added to dry THF (15 mL). The reaction mixture was stirred at 50 °C for 3 h. The solvent was evaporated under reduced pressure and the residue was partitioned between aqueous $NaHCO_3$ (25 mL) and ethyl acetate (25 mL). The organic solvent was separated and dried over anhydrous Na_2SO_4. The crude product was purified by silica gel flash chromatography, using dichloromethane–methanol (9:1), to yield the corresponding thioamide as a yellow solid (82 mg, 54%). The solid (76 mg, 0.5 mmol), 3-(bromoacetyl)pyridine hydrobromide (**7**, 140 mg, 0.50 mmol), and cesium carbonate (165 mg, 0.50 mmol) were added to dry DMF (10 mL). The reaction mixture was heated at 100 °C for 8 h and then allowed to cool. The reaction mixture was quenched with distilled water (30 mL). The organic materials were extracted using ethyl acetate (30 mL). The organic layer was isolated and dried over anhydrous Na_2SO_4. The solvent was evaporated under reduced pressure. The solid residue was purified by silica gel flash chromatography, using dichloromethane–methanol (95:5), to yield a brownish-white solid (70 mg, 56%): mp 104–105 °C. ^{1}H NMR ($CDCl_3$) δ 9.18 (d, J = 1.8 Hz, 1H), 8.57 (m, 2H), 8.52 (d, J = 5.1 Hz, 1H), 8.21 (dt, J = 1.8, 8.1 Hz, 1H), 7.71 (d, J = 4.8 Hz, 1H), 7.70 (s, 1H), 7.34 (dd, J = 5.1, 8.1 Hz, 1H), 2.66 (s, 3H); ^{13}C NMR ($CDCl_3$) δ 165.38, 153.25, 152.81, 149.36, 147.83, 147.73, 138.80, 133.58, 130.55, 129.79, 123.62, 122.43, 115.44, 18.88; EIMS (m/z, rel intensity) 253 (M^+, 100); HRMS (EI), m/z M^+ 253.0678, calcd for $C_{14}H_{11}N_3S$ 253.0674; HPLC purity (C-18 reverse phase column): 96.10% (methanol–H_2O, 95:5).

4.8. General procedure for thiazoles 19 and 20

The appropriate thioamide (thionicotinamide or thioisonicotinamide, 60 mg, 0.5 mmol), 2-bromo-1-(6-bromopyridin-3-yl) ethanone (**18**, 140 mg, 0.50 mmol), and cesium carbonate (175 mg, 0.52 mmol) were added to dry DMF (10 mL). The reaction mixture was heated at 120 °C for 6 h then allowed to cool and was quenched with distilled water (30 mL). The organic materials were extracted in a separatory funnel using ethyl acetate (30 mL). The organic layer was isolated and dried over anhydrous Na_2SO_4. Solvent was evaporated under reduced pressure. The solid residue was purified by silica gel flash chromatography, using a gradient of dichloromethane–methanol concentrations (95:5 then 9:1), to yield the desired compounds.

4.8.1. 4-(6-Bromopyridin-3-yl)-2-(pyridin-4-yl)thiazole (19)

Yellowish-brown solid (89 mg, 55%): mp >300 °C. ^{1}H NMR ($CDCl_3$) δ 8.95 (d, J = 2.1 Hz, 1H), 8.75 (d, J = 8.0 Hz, 2H), 8.16 (dd, J = 2.4, 7.4 Hz, 1H), 7.87 (d, J = 8.0 Hz, 2H), 7.71 (s, 1H), 7.59 (dd, J = 0.6, 7.4 Hz, 1H); ^{13}C NMR ($CDCl_3$) δ 163.44, 153.49, 149.06 (2C), 146.02, 145.63, 142.17, 137.79, 129.62, 129.30, 123.57, 123.18 (2C); ESIMS (m/z, rel intensity) 320/318 (MH^+, 100/88); HRMS (ESI), m/z MH^+ 317.9708, calcd for $C_{13}H_9BrN_3S$ 317.9701; HPLC purity (C-18 reverse phase column): 97.22% (methanol–H_2O, 95:5).

4.8.2. 4-(6-Bromopyridin-3-yl)-2-(pyridin-3-yl)thiazole (20)

Yellowish-brown solid (95 mg, 57%): mp >300 °C. ^{1}H NMR ($CDCl_3$) δ 9.23 (d, J = 1.8 Hz, 1H), 8.95 (d, J = 2.1 Hz, 1H), 8.70 (d, J = 3.6 Hz, 1H), 8.32 (d, J = 8.1 Hz, 1H), 8.16 (dd, J = 2.4, 8.1 Hz, 1H), 7.65 (s, 1H), 7.58 (d, J = 8.4 Hz, 1H), 7.44 (dd, J = 4.8, 7.8 Hz, 1H); ^{13}C NMR ($CDCl_3$) δ 165.41, 152.35, 151.20, 147.88, 147.74, 141.53, 136.21, 133.69, 129.24, 129.17, 128.12, 123.78, 114.87; ESIMS (m/z, rel intensity) 320/318 (MH^+, 97/100); HRMS (ESI), m/z MH^+ 317.9705, calcd for $C_{13}H_9BrN_3S$ 317.9701; HPLC purity (C-18 reverse phase column): 96.50% (methanol–H_2O, 95:5).

4.9. Preparation of 21–23

Bromopyridines **19** or **20** (30 mg, 0.1 mmol) and sodium methoxide (26 mg, 0.5 mmol) were added to absolute methanol (2 mL) in a sealed tube. In the case of **22**, absolute ethanol was used. The reaction mixture was heated at 120 °C for 8 h and then allowed to cool. The solvent was evaporated under reduced pressure and the solid residue was partitioned between ethyl acetate (10 mL) and water (10 mL). The organic layer was isolated and dried over anhydrous Na_2SO_4. The solvent was evaporated under reduced pressure and the solid residue was purified by silica gel flash chromatography, using dichloromethane–methanol (95:5), to yield the products as solids.

4.9.1. 4-(6-Methoxypyridin-3-yl)-2-(pyridin-4-yl)thiazole (21)

Off-white solid (15 mg, 58%): mp 180 °C. ^{1}H NMR ($CDCl_3$) δ 8.95 (d, J = 2.4 Hz, 1H), 8.72 (d, J = 7.8 Hz, 2H), 8.15 (d, J = 7.4 Hz, 2H), 7.88 (s, 1H), 7.71 (s, 1H), 7.52 (dd, J = 0.6, 7.4 Hz, 1H), 3.99 (s, 3H); ^{13}C NMR ($CDCl_3$) δ 163.77, 150.68 (2C), 147.91, 145.04, 136.87, 136.23, 128.16, 120.27 (2C), 115.85, 113.27, 110.90, 53.63; ESIMS (m/z, rel intensity) 270 (MH^+, 100); HRMS (ESI), m/z MH^+ 270.0704, calcd for $C_{14}H_{12}N_3OS$ 270.0701; HPLC purity (C-18 reverse phase column): 99.39% (methanol–H_2O, 9:1).

4.9.2. 4-(6-Ethoxypyridin-3-yl)-2-(pyridin-4-yl)thiazole (22)

White solid (12 mg, 46%): mp 125–126 °C. ^{1}H NMR ($CDCl_3$) δ 8.74 (m, 3H), 8.14 (d, J = 1.8 Hz, 1H), 8.15 (d, J = 7.8 Hz, 2H), 7.50 (s, 1H), 6.80 (d, J = 8.0 Hz, 1H), 4.40 (q, J = 6.9 Hz, 2H), 1.41 (t, J = 6.9 Hz, 3H); ^{13}C NMR ($CDCl_3$) δ 165.18, 163.88, 154.37, 150.67 (2C), 145.08, 140.12, 136.81, 123.44, 120.24 (2C), 113.13, 110.97, 61.97, 14.61; ESIMS (m/z, rel intensity) 284 (MH^+, 100); HRMS (ESI), m/z MH^+ 284.0855, calcd for $C_{15}H_{14}N_3OS$ 284.0858; HPLC purity (C-18 reverse phase column): 96.73% (methanol–H_2O, 95:5).

4.9.3. 4-(6-Methoxypyridin-3-yl)-2-(pyridin-3-yl)thiazole (23)

White solid (12 mg, 47%): mp 129–130 °C. ^{1}H NMR ($CDCl_3$) δ 9.22 (d, J = 2.1 Hz, 1H), 8.77 (d, J = 2.4 Hz, 1H), 8.66 (dd, J = 1.8, 6.0 Hz, 1H), 8.29 (dt, J = 1.8, 6.0 Hz, 1H), 8.15 (dd, J = 2.4, 8.7 Hz, 1H), 7.44 (s, 1H), 7.28 (dd, J = 1.8, 8.7 Hz, 1H), 6.82 (d, J = 8.7 Hz, 1H), 3.98 (s, 3H); ^{13}C NMR ($CDCl_3$) δ 164.69, 164.02 (2C), 153.87, 150.88, 147.70, 144.98, 136.83, 133.56, 129.49, 123.70, 112.21, 110.83, 53.61; ESI MS (m/z, rel intensity) 270 (MH^+, 100); HRMS (ESI), m/z MH^+ 270.0699, calcd for $C_{14}H_{12}N_3OS$ 270.0701; HPLC purity (C-18 reverse phase column): 98.01% (methanol–H_2O, 9:1).

4.10. Molecular modeling

Compounds of interest were built with Sybyl 7.1 software and minimized to 0.01 kcal/mol by the Powell method, using Gasteiger–Hückel charges and the Tripos force field. The energy-optimized compounds were docked into the androgen binding pocket in aromatase after removal of the structure of the natural ligand. The parameters were set as the default values for GOLD. The maximum distance between hydrogen bond donors and acceptors for hydrogen bonding was set at 3.5 Å. After docking, the first pose conformations of compounds of interest were merged into the ligand–free protein. The new ligand–protein complex was subsequently subjected to energy minimization using the Amber force field with Amber charges. During the energy minimization, the structure of the compounds of interest and a surrounding 10 Å sphere of the protein were allowed to move. The structure of the remaining protein was kept frozen. The energy minimization was performed using the Powell method with a 0.05 kcal/(mol Å) energy gradient convergence criterion and a distance dependent dielectric function.

4.11. Biological assay

4.11.1. Aromatase assay

Aromatase activity was assayed as previously reported, with the necessary modifications to assay in a 384-well plate.[29] Briefly, the test compound (3.5 μL) was preincubated with 30 μL of NADPH-regenerating system (2.6 mM $NADP^+$, 7.6 mM glucose 6-phosphate, 0.8 U/mL glucose-6-phosphate dehydrogenase, 13.9 mM $MgCl_2$, and 1 mg/mL albumin in 50 mM potassium phosphate buffer, pH 7.4) for 10 min at 37 °C. The enzyme and substrate mixture (33 μL of 1 μM CYP19 enzyme, BD Biosciences, 0.4 μM dibenzylfluorescein, 4 mg/mL albumin in 50 mM potassium phosphate, pH 7.4) was added, and the plate was incubated for 30 min at 37 °C before quenching with 25 μL of 2 N NaOH. After termination of the reaction and shaking for 5 min, the plate was further incubated for 2 h at 37 °C. This enhances the ratio of signal to background. Fluorescence was measured at 485 nm (excitation) and 530 nm (emission). IC_{50} values were based on three independent experiments performed in duplicate using five concentrations of test substance. Letrozole, anastrozole, and fadrozole were used as positive controls.

Kinetic analyses were performed essentially as described above. Test compounds were preincubated with 30 μL of NADPH regenerating system (2.6 mM $NADP^+$, 7.6 mM glucose 6-phosphate, 0.8 U/mL glucose 6-phosphate dehydrogenase, 13.9 mM $MgCl_2$, and 1 mg/mL albumin in 50 mM potassium phosphate buffer, pH 7.4) for 10 min at 37 °C. A range of eight concentrations centered around the IC_{50} was tested for each inhibitor. Substrate was added at three concentrations: 800, 400, and 200 nM. Finally, CYP19 (1 μM) was added, and fluorescence was measured at 485 nm (excitation) and 530 nm (emission) every 10 s for at least 5 min. Michaelis–Menten and Dixon plots were used to evaluate the resulting data, and K_i values were calculated. Error limits represent three independent experiments for each compound.

Supplementary data

Supplementary data associated with this article can be found, in the online version, at doi:10.1016/j.bmc.2012.01.047.

References and notes

1. Chow, L. W.; Yip, A. Y.; Loo, W. T.; Toi, M. *Cancer Lett.* **2008**, *262*, 232. and references 1 and 2 cited therein.
2. American Cancer Society. *Brest Cancer Facts & Figures 2009–2010*; American Cancer Society, Inc.: Atlanta.
3. Chen, S.; Zhou, D.; Okubo, T.; Kao, Y. C.; Eng, E. T.; Grube, B.; Kwon, A.; Yang, C.; Yu, B. *Ann. N.Y. Acad. Sci.* **2002**, *963*, 229.
4. Yanyan, H.; Michael, C.; Yate-Ching, Y.; Shiuan, C. *Biochem. Pharmacol.* **2008**, *75*, 1161.
5. Toniolo, P. G.; Levitz, M.; Zeleniuch-Jacquotte, A.; Banerjee, S.; Koenig, K. L.; Shore, R. E.; Strax, P.; Pasternack, B. S. *J. Natl. Cancer Inst.* **1995**, *87*, 190.
6. (a) Wiseman, L. R.; McTavish, D. *Drugs* **1993**, *45*, 66; (b) Clemett, D.; Lamb, H. M. *Drugs* **2000**, *59*, 1279.
7. Wellington, K.; Faulds, D. M. *Drugs* **2002**, *62*, 2483.
8. (a) Buzdar, A.; Douma, J.; Davidson, N.; Elledge, R.; Morgan, M.; Smith, R.; Porter, L.; Nabholtz, J.; Xiang, X.; Brady, C. *J. Clin. Oncol.* **2001**, *19*, 3357; (b) Eisen, A.; Trudeau, M.; Shelley, W.; Messersmith, H.; Pritchard, K. I. *Cancer Treat. Rev.* **2008**, *34*, 157.
9. Yahiaoui, S.; Fagnere, C.; Pouget, C.; Buxeraud, J.; Chulia, A. *Bioorg. Med. Chem.* **2008**, *16*, 1474.
10. (a) Plourde, P. V.; Dyroff, M.; Dowsett, M.; Demers, L.; Yates, R.; Webster, A. *J. Steroid Biochem. Mol. Biol.* **1995**, *53*, 175; (b) Bossche, V.; Koymans, M. H. *Breast Cancer Res. Treat.* **1994**, *30*, 43; (c) Mitrenga, M.; Hartmann, R. W. *Eur. J. Med. Chem.* **1995**, *30*, 241.
11. (a) Pizarro, J. G.; Verdaguer, E.; Ancrenaz, V.; Junyent, F.; Sureda, F.; Pallàs, M.; Folch, J.; Camins, A. *Neurochem. Res.* **2011**, *36*, 187; (b) Oi, N.; Jeong, C. H.; Nadas, J.; Cho, Y. Y.; Pugliese, A.; Bode, A. M.; Dong, Z. *Cancer Res.* **2010**, *70*, 9755.
12. (a) Carbó, N.; Costelli, P.; Baccino, F. M.; López-Soriano, F. J.; Argilés, J. M. *Biochem. Biophys. Res. Commun.* **1999**, *254*, 739; (b) Chen, Y.; Tseng, S. H.; Lai, H. S.; Chen, W. J. *Surgery* **2004**, *136*, 57; (c) Roy, P.; Kalra, N.; Prasad, S.; George, J.; Shukla, Y. *Pharm. Res.* **2009**, *26*, 211.
13. Jang, M.; Cai, L.; Udeani, G. O.; Slowing, K. V.; Thomas, C. F.; Beecher, C. W. W.; Fong, H. H. S.; Farnsworth, N. R.; Kinghorn, A. D.; Mehta, R. G.; Moon, R. C.; Mezzuto, J. M. *Science* **1997**, *275*, 218.
14. Dudley, J. I.; Lekli, I.; Mukherjee, S.; Das, M.; Bertelli, A. A. A.; Das, D. K. *J. Agric. Food Chem.* **2008**, *56*, 9362.
15. Aziz, M. H.; Kumar, R.; Ahmad, N. *Int. J. Oncol.* **2003**, *23*, 17.
16. Hoshino, J.; Park, E.; Kondratyuk, T. P.; Marler, L.; Pezzuto, J. M.; van Breemen, R. B.; Mo, S.; Li, Y.; Cushman, M. *J. Med. Chem.* **2010**, *53*, 5033.
17. Mayhoub, A. S.; Marler, L.; Kondratyuk, T.; Park, E.; Pezzuto, J.; Cushman, M. *Bioorg. Med. Chem.* **2012**, *20*, 510.
18. Strasser-Weippl, K.; Goss, P. E. *J. Clin. Oncol.* **2005**, *23*, 1751.
19. Ghosh, D.; Griswold, J.; Erman, M.; Pangborn, W. *Nature* **2009**, *457*, 219.
20. Verdonk, M. L.; Cole, J. C.; Hartshorn, M. J.; Murray, C. W.; Taylor, R. D. *Protein Struct. Funct. Genet.* **2003**, *52*, 609.
21. (a) Shah, A. A.; Khan, Z. A.; Choudhary, N.; Loholter, C.; Schafer, S.; Marie, G. P. L.; Farooq, U.; Witulski, B.; Wirth, T. *Org. Lett.* **2009**, *11*, 3578; (b) Cheng, D.; Chen, Z. *Synth. Commun.* **2002**, *32*, 2155; (c) Yan, M.; Chen, Z.; Zheng, Q. *J. Chem. Res. (S)* **2003**, 618; (d) Patil, P. C.; Bhalerao, D. S.; Dangate, P. S.; Akamanchi, K. G. *Tetrahedron Lett.* **2009**, *50*, 5820; (e) Isobe, T.; Ishikawa, T. *J. Org. Chem.* **1999**, *64*, 6989; (f) Forlani, L.; Lugli, A.; Boga, C.; Corradi, A. B.; Sgarabotto, P. *J. Heterocycl. Chem.* **2000**, *37*, 63.
22. Howe, R. K.; Shelton, B. R. *J. Org. Chem.* **1981**, *46*, 771.
23. Chill, T. S.; Mebane, C. R. *Synth. Commun.* **2010**, *40*, 2014.
24. Nuriev, V. N.; Zyk, N. V.; Vatsadze, S. Z. *ARKIVOC* **2005**, *4*, 208.
25. Santora, V.; Askew, B.; Ghose, A.; Hague, A.; Kim, T. S.; Laber, E.; Li, A.; Lian, B.; Liu, G.; Norman, M. H.; Smith, L.; Tasker, A.; Tegley, C.; Yang, K. PCT Int. Appl., 2002014311, 2002.
26. Dunn, A. D. *Org. Prep. Proced. Int.* **1999**, *31*, 120.
27. El-Deeb, I. M.; Lee, S. H. *Bioorg. Med. Chem.* **2010**, *18*, 3860.
28. Wu, T. Y. H.; Juteau, H.; Ducharme, Y.; Friesen, R. W.; Guiral, S.; Dufresne, L.; Poirier, H.; Salem, M.; Riendeau, D.; Mancini, J.; Brideau, C. *Bioorg. Med. Chem. Lett.* **2010**, *20*, 6978.
29. Maiti, A.; Cuendet, M.; Croy, V. L.; Endringer, D. C.; Pezzuto, J. M.; Cushman, M. *J. Med. Chem.* **2007**, *50*, 2799.